Material screening and selection for XENON100

E. Aprile[a], K. Arisaka[f], F. Arneodo[c], A. Askin[b], L. Baudis[b], A. Behrens[b], K. Bokeloh[h], E. Brown[f], J.M.R. Cardoso[d], B. Choi[a],
D. Cline[f], S. Fattori[c,i], A.D. Ferella[b], K.L. Giboni[a], A. Kish[b], C.W. Lam[f], J. Lamblin[j], R.F. Lang[a], K.E. Lim[a], J.A.M. Lopes[d],
T. Marrodán Undagoitia[b], Y. Mei[e], A.J. Melgarejo Fernandez[a], K. Ni[g], U. Oberlack[i,e], S.E.A. Orrigo[d], E. Pantic[f], G. Plante[a],
A.C.C Ribeiro[d], R. Santorelli[b], J.M.F. dos Santos[d], M. Schumann[b,e], P. Shagin[e], A. Teymourian[f], D. Thers[j], E. Tziaferi[b],
H. Wang[f], C. Weinheimer[h],
(XENON100 Collaboration),
M. Laubenstein[c], S. Nisi[c]

[a]*Department of Physics, Columbia University, New York, NY 10027, USA*
[b]*Physik-Institut, Universität Zürich, 8057 Zürich, Switzerland*
[c]*INFN – Laboratori Nazionali del Gran Sasso, 67010 Assergi, Italy*
[d]*Department of Physics, University of Coimbra, R. Larga, 3004-516, Coimbra, Portugal*
[e]*Department of Physics & Astromony, Rice University, Houston, TX, 77251, USA*
[f]*Department of Physics & Astromony, University of California, Los Angeles, CA, 90095, USA*
[g]*Shanghai Jiao Tong University, Shanghai, China*
[h]*Institut für Kernphysik, Universität Münster, 48149 Münster, Germany*
[i]*Institut für Physik, Johannes Gutenberg-Universität Mainz, 55099 Mainz, Germany*
[j]*SUBATECH, Ecole des Mines de Nantes, Université de Nantes, CNRS/IN2P3 Nantes, France*

Abstract

Results of the extensive radioactivity screening campaign to identify materials for the construction of XENON100 are reported. This Dark Matter search experiment is operated underground at Laboratori Nazionali del Gran Sasso (LNGS), Italy. Several ultra sensitive High Purity Germanium detectors (HPGe) have been used for gamma ray spectrometry. Mass spectrometry has been applied for a few low mass plastic samples. Detailed tables with the radioactive contaminations of all screened samples are presented, together with the implications for XENON100.

Keywords: Dark Matter, Material Screening, Low Activity, HPGe

1. Introduction

The indirect evidence of a significant cold dark matter component in the Universe [1, 2, 3] motivated the start of several experiments aiming to directly detect Dark Matter in the form of Weakly Interacting Massive Particles (WIMPs) [4, 5, 6]. The possible existence of WIMPs is supported by beyond-Standard Model theories such as supersymmetric theories (SUSY), models with extra dimensions and little Higgs models [7, 8, 9, 10]. Several experiments are aiming to directly detect WIMP dark matter by searching for the elastic scattering of WIMPs off target nuclei. XENON100, which has recently published one of the best limits on spin-independent WIMP-nucleon scattering cross sections [11, 12], is one of the most sensitive experiments of the current generation. It is a double-phase (liquid/gas) time projection chamber (TPC) [13], which allows fiducialization of the active target and discrimination of the nuclear recoil signal from electronic recoils, induced by background radiation. The former is made possible by a reconstruction of the interaction vertex in three dimensions, whereas the latter is possible because of the different charge to scintillation light ratio for the two types of interaction [14].

In order to reach its design sensitivity, the experiment is to be built from materials with a very low intrinsic radioactivity. Therefore, the radioactive screening and selection of materials has played an important role in the design and during the construction phase of XENON100, as well as in the background simulation of the experiment [15]. The XENON collaboration used the High Purity Germanium (HPGe) detector Gator [16], operated by the University of Zurich, to perform gamma ray spectrometry in order to determine the intrinsic radioactivity of materials considered for the construction of XENON100. Moreover, HPGe detectors of the low-level counting facility at Laboratori Nazionali del Gran Sasso (LNGS), Italy, [17] were also used. This facility includes the GeMPI-I and GeMPI-II detectors, which are the most sensitive low-radioactivity HPGe detectors in the world [18]. The radioactivity of a few low-mass samples has been determined by mass spectroscopy.

This paper is organized as follows: First the radiopurity requirements of experiments searching for Dark Matter are reviewed, followed by a short description of the methods used for the sample screening in Sections 3 and 4. The results are presented and discussed in Section 5.

---

2. Radiopurity Requirements for direct Dark Matter Searches and XENON100

Experiments searching for Dark Matter are often limited by background radiation from the detector materials and surroundings, including a possible radiation shield, and by interactions induced by cosmic rays, especially muons.

Generally, particles can interact either with the atomic electrons of the detector material (electronic recoils) or with the target nuclei (nuclear recoils). Since the electrically neutral WIMPs and neutrons are both expected to produce nuclear recoils, neutrons are the most dangerous background for Dark Matter experiments, as they can potentially mimic a WIMP signal. In most cases, however, the dominating background is from electronic recoils. For this reason, most experiments employ at least one technique to discriminate between nuclear and electronic recoils.

The dominant electronic recoil background usually comes from γ-rays from radioactive isotopes in the shield and in the detector itself. β-decays only contribute when they occur in the target or at the target's surface. Depending on the energy of the electrons, they can generate Bremsstrahlung in the vicinity of the sensitive volume, which might add an additional source of background. α-decays do not directly contribute to the background at low energies, given the typical α energies of > 3 MeV. However, they might indirectly contribute to the nuclear recoil background, as they can produce neutrons in (α, n) reactions and cause nuclear recoils from daughter nuclei. Another source of neutrons is from spontaneous fission of ^{238}U.

The most relevant sources of radioactive contamination in the XENON100 experiment are primordial radionuclides (^{238}U, ^{232}Th and ^{40}K), anthropogenic radionuclides (^{137}Cs, ^{85}Kr), cosmogenic radionuclides (mainly ^{60}Co) and environmental radioactive noble gases, such as ^{222}Rn and ^{220}Rn which are daughters of the ^{238}U and ^{232}Th decay chains.

The goal of the XENON100 experiment is to probe spin-independent WIMP-nucleon scattering cross sections down to the level of $\sim 2 \times 10^{-45}$ cm^2. In order to reach this sensitivity, one of the key requirements on the experiment design is the suppression of background and a total electronic recoil background of $< 10^{-2}$ events keV^{-1} kg^{-1} day^{-1} is required. This is achieved by shielding the detector from environmental radioactivity with a passive shield, by the detector design using an active LXe veto scintillator, fiducial volume cuts, and by constructing the detector from materials with a low intrinsic radioactivity [15].

3. Gamma Ray Spectrometry with HPGe Detectors

When measuring the intrinsic radioactivity of a sample material with high purity germanium (HPGe) detectors, one exploits the excellent energy resolution of these detectors, together with the very low background spectrum of dedicated counting setups. This allows to identify radioactive contaminations by identification of the γ-lines from their decay [19]. The spectrometers used for the measurements presented here are installed underground at LNGS, at a depth of 3100 meters water equivalent relative to a flat overburden, where the muon flux is

reduced by a factor $\sim 10^6$ with respect to above ground. This also reduces the neutron flux by several orders of magnitude since the hadronic showers from cosmic rays are completely blocked and muon induced neutrons are strongly suppressed. The remaining neutron flux is mainly due to fission and (α, n) reactions. A ventilation system constantly brings fresh air from the outside to the laboratory, leading to a rather constant ^{222}Rn concentration of ~30 Bq/m^3 at the location of the HPGe spectrometers.

In this section we briefly describe the facilities used for this study and how the measurements were analyzed.

Gator Facility. Gator [16] is a High Purity p-type coaxial germanium detector of 2.2 kg sensitive mass, a relative efficiency of 100.5%[1] and a measured resolution of ~ 3 keV FWHM at 1332 keV. In order to ensure high detection sensitivies, the detector and its shield have been constructed using materials selected for their extremely low intrinsic radioactive contaminations. The shield of Gator fulfills the crucial requirements of having sufficient sample capacity and low intrinsic background, and uses nitrogen purging against radon and its progenies. The inner dimensions of the sample cavity are $25 \times 25 \times 33$ cm^3, with the detector reaching into the cavity. The total available volume is ~19 liters. An example measurement, showing the different gamma lines for the spectrum of a sample measured with Gator, is shown in Fig. 1.
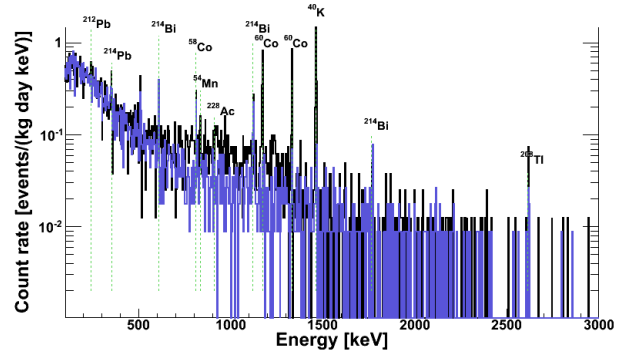

Figure 1: Example of a measurement with Gator: 7 *Hamamatsu* R8520 PMTs were screened (entry 34 in Table 1). The lines from their intrinsic radioactive contaminations (solid black) are clearly visible above the Gator background spectrum (blue).

LNGS Counting Facility. The low background germanium counting facility of LNGS [17] is equipped with several high-purity coaxial germanium detectors with large sensitive volumes, low intrinsic background and high energy resolution (< 2.6 keV FWHM at 1332 keV). They include GeMPI-I and GeMPI-II [18], the most sensitive screening facilities worldwide. For all detectors and shields, only selected materials with lowest intrinsic radioactivity have been used. The sample cavities have volumes which range from one liter up to 15 liters (GeMPI-I/II).

---

[1]The efficiency is defined relative to a 7.62 cm × 7.62 cm NaI(Tl) crystal, for the 1.33MeV ^{60}Co photopeak, at a source-detector distance of 25cm [21].

Measurement. In order to increase the sensitivity of a γ-counting measurement, it is beneficial to use massive samples. Since placing the samples very close to the detector also increases the efficiency, the best configuration is to place the sample on top of the germanium crystal. For large or heavy samples, however, this requirement cannot always be fulfilled and the sample has to be placed around the detector.

Before the measurement, the samples are properly cleaned from surface contaminations in an ultrasonic bath of pure ethanol (> 98%). Afterwards they have been stored in an environment purged with pure boil-off N_2 for several days in order to let ^{222}Rn and its progenies decay or diffuse out. Once the samples are inserted into the spectrometers, the γ-ray spectra are acquired automatically using standard multi-channel analyzers. The measurement time varied according to the sample. Typically it was in the range of days to several weeks. Data analysis has been performed off-line after the measurement.

As the geometrical arrangement of every sample is unique, the detection efficiency has been calculated for every measurement using Monte Carlo simulations. For Gator, the GEANT4 toolkit [20] is used, while the LNGS facility detectors employ simulations based on GEANT4, GEANT3.21 and EGS4 (Electrons Gamma Showers). In all cases, the whole sample and detector geometry is coded. Standard sources of known activity are regularly used to test the reliability of this method of efficiency estimation, giving excellent agreement [16].

Analysis. To determine the concentration of a specific radioactive decay chain, the characteristic γ-lines of the chains are considered:
– ^{232}Th chain: ^{228}Ac, ^{212}Pb, ^{212}Bi and ^{208}Tl.
– ^{238}U chain: ^{234m}Pa, ^{234}Th, ^{214}Pb and ^{214}Bi.
– ^{235}U chain: ^{235}U.
In some cases the activity of ^{235}U is deduced from that of ^{238}U by taking into account their relative abundance in natural uranium (0.70% of ^{235}U and 99.27% of ^{238}U). The activities of the different decay chains are calculated taking into account the mass of the sample, the measurement time, the efficiency from the Monte Carlo simulation and the number of counts in the characteristic γ-line. The background spectrum, which is measured regularly and the Compton continuum from other lines are subtracted. More details on the analysis can be found in [16]. Upper limits are calculated using the method introduced in [22] for Gator and in [23] for the LNGS screening facility.

Secular equilibrium can be verified for ^{232}Th because of the relatively high branching ratios of the γ-lines emitted in the initial part of the chain. For most of the screened samples this is not possible for ^{238}U. However, upper limits obtained from the γ-lines of the daughters ^{234m}Pa and ^{234}Th do not exclude the secular equilibrium hypothesis. The only samples for which a break in the secular equilibrium of ^{238}U has been detected are the field shaping resistors and the ceramic feedthrough (entries 44 and 46 in Table 1): the radioactivity of the different parts of the decay chain are given explicitly there.

All other relevant radioactive nuclides contributing to the γ-ray spectra (such as ^{40}K, ^{60}Co, ^{137}Cs, etc.) are analyzed using their most prominent γ-lines at specific energies and branching ratios.

4. Inductively Coupled Plasma Mass Spectrometry

For a few plastic samples, with a total mass too small to yield reasonable sensitivity with the HPGe detectors, inductively coupled Plasma-Mass Spectrometry (ICP-MS) has been used to determine the intrinsic radioactivity. The ICP-MS 7500a from *Agilent Technologies* employed here is a quadrupolar mass spectrometer using an argon plasma torch (ICP-torch) to ionize the sample.

Before the procedure, the samples are cleaned and prepared as described in Section 3. They are then ashed at 600°C, using the dry ashing procedure described in [24] and dissolved in a 10% ultra pure nitric acid solution, which is nebulized in a spray chamber where it forms an aerosol. The aerosol is atomized and ionized by the ICP-torch, producing a cloud of positively charged ions. The ions are extracted from the plasma into an ultra high vacuum system containing a quadrupole analyzer, where they are separated according to their mass-to-charge ratio q. The count rate obtained for a particular q is compared with a calibration curve to determine the concentration of the elements in the sample.

For the samples screened with the ICP-MS secular equilibrium is assumed.

5. Results and Discussion

The main results from the screening campaign are presented in Table 1. It lists the material, the supplier and its use in the XENON100 experiment (see also Section 5.5). It provides details on the measurement (detector, measurement time and sample mass) and gives the measured radioactive contaminations or, where no spectral lines have been observed, upper limits at 95% confidence level. In this Section, the most relevant results are discussed.

5.1. Metal Samples

Lead is used for the XENON100 passive shield. Material from two different suppliers was screened (entries 1-4 in Table 1). The lead from *Plombum FL* is a standard lead while the one from *Founderies de Gentilly* has a low contamination of ^{210}Pb. This was confirmed in both HPGe facilities, however, measured with different sample masses. When evident lines are detected, the results are in agreement, when only upper limits can be given, the limits from the measurement with more mass are considerably lower. The ^{210}Pb activities are (530±70) Bq/kg and (26 ± 6) Bq/kg for lead with high and low ^{210}Pb contamination, respectively.

Table 1: Screening Results. See text for discussion.

	Material	Supplier	Use	Detector	Time [d]	Amount	Unit	228Ra	228Th	238U	226Ra	235U	40K	137Cs	60Co
	Metal														
1.	Lead	Plombum	Outer Pb shield	Gator	18.4	2.27 kg	mBq/kg	< 6.9	< 0.52	< 260	< 4.2	< 12	14(3)	< 0.81	< 0.11
2.	Lead	Plombum	Outer Pb shield	LNGS	14.5	44 kg	mBq/kg	< 6.6	< 1.6	< 130	< 5.7	< 51	14(6)	< 2.1	< 1.1
3.	Lead	Foundaries de Gentilly	Inner Pb shield	Gator	17.8	2.27 kg	mBq/kg	< 0.66	< 0.42	< 24	< 0.71	< 1.8	< 1.46	0.63(6)	< 0.11
4.	Lead	Foundaries de Gentilly	Inner Pb Shield	LNGS	18.7	44 kg	mBq/kg	< 3.9	< 4.3	< 33	< 6.8	< 20	< 28	< 0.85	< 0.19
5.	Copper	Nordeutsche Affinerie	Shield	Gator	51.4	512 kg	μBq/kg	21(7)	21(7)	70(20)	70(20)	3.4	23(6)		2(1)
6.	Copper	Nordeutsche Affinerie	TPC	Gator	20.3	18.1 kg	mBq/kg	< 0.37	< 0.33	< 11	< 0.37	< 0.47	< 1.3	< 0.14	0.24(6)
7.	Stainless Steel 316Ti (1.5 mm)	NIRONIT	Cryostat wall	LNGS	6.87	1.2 kg	mBq/kg	< 2.4	< 1.0	< 130	< 1.9	< 2.0	10(4)	< 0.9	8.5(9)
8.	Stainless Steel 316Ti (2.5 mm)	NIRONIT	Cryostat bottom	LNGS	20.6	1.97 kg	mBq/kg	< 3.1	< 1.5	< 42	< 2.7	< 1.4	< 12	< 0.88	13(1)
9.	Stainless Steel 316Ti (3.0 mm)	NIRONIT	Grid frame	Gator	6.76	6.6 kg	mBq/kg	< 4.1	< 1.8	< 130	3.6(8)	< 5.8	< 5.7	< 1.1	7(1)
10.	Stainless Steel 316Ti (25 mm)	NIRONIT	Top flange/ Support bars	LNGS	5.58	1.52 kg	mBq/kg	< 0.92	2.9(7)	< 20	< 1.3	< 1.3	< 7.1	< 0.82	1.4(3)
11.	Screws 2-56 7/16"	McMaster	Standard screw	Gator	12.1	0.27kg	mBq/kg	24(5)	< 21	< 550	< 13	< 25	< 47	< 5.1	6(2)
	Plastic														
12.	Polyethylene	in2plastic	Shield wall	Gator	5.85	2.76 kg	mBq/kg	< 5.4	< 3.7	< 170	< 5.1	< 7.6	< 14	< 1.7	< 1.4
13.	Polyethylene	in2plastic	Shield door	Gator	3.12	3.1 kg	mBq/kg	< 4.3	< 5.8	< 220	< 6.5	< 9.9	< 13	< 2.1	< 1.7
14.	Polyethylene	in2plastic	Shield wall/door	LNGS	28.9	8.44 kg	mBq/kg	< 0.094	< 0.14	< 3.8	0.23(5)	< 0.37	0.7(4)	0.06(3)	
15.	PTFE	Maagtechnic	TPC	Gator	14.35	13.5 kg	mBq/kg	< 0.39	< 0.16	< 6.2	< 0.31	< 0.28	< 2.25	< 0.13	< 0.11
16.	PTFE	Maagtechnic	TPC	Gator	47.4	23.5 kg	mBq/kg	< 0.16	< 0.10	< 3.0	< 0.06	< 0.13	< 0.75	< 0.07	< 0.03
17.	PTFE	McMaster	Veto reflector	ICP-MS		5.1 g	mBq/kg	0.5(1)	0.5(1)	0.25(5)	0.25(5)	0.011(2)	< 3.1		
18.	PTFE	McMaster	XENON10 TPC	LNGS	10.1	0.23 kg	mBq/kg	< 1.8	< 2.3	< 36	< 1.1	< 1.4	< 7.6	< 0.44	
19.	PTFE	APT	Not used	LNGS	23.5	6.54 kg	mBq/kg	< 0.15	< 0.13	< 12	< 0.16	< 0.59	3(1)	< 0.11	0.15(7)

Table 1: Screening Results (continued).

#	Material	Supplier	Use	Detector	Unit	Time [d]	Amount	^{228}Ra	^{228}Th	^{238}U	^{226}Ra	^{235}U	^{40}K	^{137}Cs	^{60}Co
Light Sensors															
20.	R8520 - Batch 1	Hamamatsu	Top array, veto	LNGS	11.6	7 pc	mBq/PMT	< 0.32	0.19(3)	< 5.3	0.15(3)	< 0.13	10(1)	< 0.05	0.56(5)
21.	R8520 - Batch 2	Hamamatsu	Bottom array	LNGS	21.6	7 pc	mBq/PMT	< 0.22	0.16(4)	< 5.2	0.21(3)	0.10(4)	9(1)	< 0.05	0.59(5)
22.	R8520 - Batch 3	Hamamatsu	Not used	LNGS	6.65	1 pc	mBq/PMT	< 2.1	1.9(5)	< 75	0.6(1)	< 0.70	120(10)	0.51	4.5(5)
23.	R8520 - Batch 4	Hamamatsu	Top array	LNGS	18.4	7 pc	mBq/PMT	< 0.23	0.19(3)	< 2.6	0.25(4)	< 0.08	7(1)	< 0.05	0.67(6)
24.	R8520 - Batch 5	Hamamatsu	Not used	LNGS	12.8	4 pc	mBq/PMT	< 0.49	0.38(8)	< 9.9	0.25(4)	< 0.08	7(1)	< 0.05	0.67(6)
25.	R8520 - Batch 6	Hamamatsu	Not used	LNGS	10.4	5 pc	mBq/PMT	< 0.42	0.38(8)	< 9.9	0.39(8)	< 0.24	12(2)	17(6)	2.7(2)
26.	R8520 - Batch 7	Hamamatsu	Top/bottom array, veto	LNGS	24.4	39 pc	mBq/PMT	0.087(3)	0.11(1)	< 4.7	0.12(1)	0.04(1)	6.9(7)	0.027(7)	1.5(1)
27.	R8520 - Batch 8	Hamamatsu	Top array, veto	LNGS	11.9	48 pc	mBq/PMT	< 0.11	0.11(1)	< 1.4	0.12(1)	0.04(1)	7.7(8)	< 0.020	0.56(4)
28.	R8520 - Batch 9	Hamamatsu	Bottom array	LNGS	4.7	23 pc	mBq/PMT	0.5(2)	0.22(4)	< 2.7	0.16(5)	< 0.073	14(2)	< 0.021	0.73(7)
29.	R8520 - Batch 10	Hamamatsu	Bottom array	Gator	5.5	22 pc	mBq/PMT	< 0.59	0.3(1)	< 15	< 0.28	< 0.67	11(1)	< 0.1	0.536(36)
30.	R8520 - Batch 11	Hamamatsu	Veto	LNGS	17.1	15 pc	mBq/PMT	0.19(3)	0.21(3)	< 2.5	0.20(3)	< 0.12	11(1)	< 0.054	2.8(2)
31.	R8520 - Batch 12	Hamamatsu	Bottom array	Gator	9.34	12 pc	mBq/PMT	< 0.70	< 0.45	< 15	< 0.36	< 0.68	14(2)	< 0.15	0.66(7)
32.	R8520 - Batch 13	Hamamatsu	Top array	LNGS	11.9	10 pc	mBq/PMT	< 0.13	0.14(3)	< 1.5	0.38(6)	< 0.062	10(1)	< 0.017	0.46(5)
33.	R8520 - Batch 14	Hamamatsu	Bottom array	LNGS	5.12	4 pc	mBq/PMT	< 0.33	< 0.15	< 13	0.14(7)	< 0.28	6(1)	< 0.13	0.57(9)
34.	R8520 - Batch 15	Hamamatsu	Bottom array	Gator	9.51	7 pc	mBq/PMT	< 0.97	< 0.60	< 22	< 0.48	< 0.99	13(2)	< 0.20	0.6(2)
35.	R8520 - Batch 16	Hamamatsu	Bottom array, veto	Gator	5.6	11 pc	mBq/PMT	< 1.1	0.3(1)	< 21	< 0.56	< 0.94	13(2)	< 0.22	0.7(1)
36.	R8520 - Batch 17	Hamamatsu	Top/bottom array	LNGS	10.4	5 pc	mBq/PMT	< 0.32	0.30(7)	< 5.8	0.20(5)	< 0.11	6(1)	< 0.13	1.3(1)
37.	QUPIDs	Hamamatsu/ UCLA	R&D for XENON	Gator	60.0	5 pc	mBq/QUPID	<0.4	0.4(2)	< 17	0.3(1)	< 0.76	5.5(6)	< 0.21	< 0.18
38.	R11410-MOD	Hamamatsu	R&D for XENON	Gator	20.4	1pc	mBq/PMT	< 3.8	< 2.6	< 95	< 2.4	< 4.3	13(4)	< 1.3	3.5(6)
39.	R11410	Hamamatsu	R&D for XENON	LNGS	11.9	1pc	mBq/PMT	< 2.7	3.0(6)	50(20)	6.1(7)	3.1(7)	50(8)	< 0.38	8.4(8)
Connections, Cables, etc.															
40.	R8520 PMT base	Custom	PMT base	LNGS	6.0	48 pc	mBq/base	0.10(2)	0.07(2)	< 3	0.16(2)	0.13(3)	< 0.16	< 0.015	< 0.010
41.	PMMA-PFA optical fiber	Luceat	PMT calibration	ICP-MS		5.0 g	mBq/kg	6(2)	6(2)	< 1.9	< 1.9	< 0.085	40(8)		
42.	Coaxial cable (RG174)	Caburn-MDC	PMT Signal	LNGS	5.0	100 m	μBq/m	20(10)	< 19	< 180	< 8.9	< 14	200(80)	< 12	< 3.9
43.	Kapton cable (1-CC-0712)	Caburn-MDC	PMT High Voltage	LNGS	14.0	79.6 g	mBq/kg	< 8.0	< 11	< 350	< 11	< 8.4	610(80)	< 5.0	< 3.5
44.	Surface mount precision plate, SM5D, 700MΩ resistors	Japan Finechem	TPC; drift field shaping	LNGS	20.8	30 pc	mBq/pc	< 0.015	0.014(3)	0.6(2)	0.027(3)	0.013(4)	0.19(3)	< 0.004	< 0.003
Vacuum Parts															
45.	Ceramic RO4350B prepreg feedthrough	Rogers Corporation	Not used	Gator	4.9	0.014kg	Bq/kg	11(1)	11(1)	9(1)	9(1)		2(1)		< 2
46.	Ceramic Feedthrough	Caburn-MDC	Electrical feedthrough	LNGS	12.8	0.586 kg	mBq/kg	13(6)	18(6)	210(90)	13(3)	< 5	< 49	< 5	21(2)
47.	Stainless Steel Flange	Caburn-MDC	Feedthrough flange	LNGS	22.3	0.495 kg	mBq/kg	7(2)	9(2)	< 83	7(2)	< 4	< 36	< 4	6(1)
Environment															
48.	Concrete	LNGS	LNGS wall	Gator	0.71	0.035 kg	Bq/kg	2.4(8)	3.8(8)	< 160	15(2)	< 7.2	42(6)	0.8(2)	< 0.70
49.	Concrete	LNGS	LNGS floor	Gator	0.23	0.033 kg	Bq/kg	7(2)	8(2)	< 190	26(5)	< 8.5	170(30)	0.9(3)	< 0.58

One of the most radiopure metals which is commonly available is oxygen-free high-conductivity (OFHC) copper. This makes it a very interesting candidate to be used for the innermost structural parts of low background detectors and it is a very pure material for shielding. Large samples of copper typically give null results, even in the most sensitive spectrometers available [18]. The copper used in the XENON100 shield (entry 5 in Table 1) is the same as used in the shield of the Gator spectrometer. From the detailed background model of this facility, copper activities of (75 ± 14) μBq/kg for ^{226}Ra and (21 ± 7) μBq/kg for ^{232}Th have been determined [16]. Of all samples presented in this paper, where a detection can be claimed, these are the ones with the lowest radioactivity contaminations.

The second copper sample in the Table (entry 6) is from the same provider (*Norddeutsche Affinerie AG*) and its radioactive contamination with ^{226}Ra and ^{232}Th is below the sensitivity of the spectrometer. At the time of the screening, it had, however, a non negligible concentration of ^{60}Co since it had been stored at the Earth's surface for several months where it was activated by cosmic rays.

Several samples of austenitic[2] stainless steel type 1.4571 (316Ti), all supplied by *NIRONIT Edelstahlhandel GmbH & Co. KG*, were screened and confirm the results published in [25] (entries 7–10). The sample sheets had a different thickness. The content of ^{226}Ra and ^{232}Th in all samples is below 4 mBq/kg. Lines were detected only in the 3 mm and 25 mm thick samples (entries 9 and 10, respectively) which had the largest sample mass. This is in agreement with [25]. The contamination of ^{60}Co is even lower than the measurements presented there. The values range from (1.4 ± 0.3) mBq/kg to (13 ± 1) mBq/kg, which are the lowest values ever published for stainless steel. Radioactivity generated by cosmic ray activation during surface exposure was detected in all the samples, with the longest lived isotope being ^{54}Mn ($\tau_{1/2}$ = 312 days) which was found with activities ranging from (1.7 ± 0.4) mBq/kg in the 25 mm sample to (0.5 ± 0.2) mBq/kg in the 2.5 mm sample.

5.2. Plastic Samples

In direct Dark Matter detection experiments, polyethylene (entries 12–14) is commonly used as neutron moderator in radiation shields surrounding the experiments. The polyethylene from the XENON100 shield was measured in different quantities and for different measurement times. All measurements are compatible with each other. ^{226}Ra, ^{40}K and ^{137}Cs are detected when a large sample (8.44 kg) is measured for a relatively long time (28.9 days), but the respective contaminations are all below 0.7 mBq/kg. However, following these results it was decided to add a 5 cm layer of OFHC copper to the XENON100 shield, inside the Polyethylene, in order to suppress this γ-background.

Polytetrafluoroethylene (PTFE, Teflon) is a material widely used in liquid xenon applications because of its physical, mechanical, dielectric and optical properties. It withstands liquid

xenon (LXe) temperatures ($-95°$C) and is a good insulator with a dielectric constant very similar to LXe (ϵ_r = 2). It also is an excellent reflector for VUV light at the xenon scintillation wavelength λ = 178 nm [26].

A possible drawback of using PTFE in Dark Matter experiments is that fluorine ^{19}F, the main component of the PTFE, has a high cross section for (α, n) reactions ($\sim$ 200 mb for E_α = 5.5 MeV [29]). The α-particles for these reactions would come from the ^{226}Ra and ^{232}Th chains from intrinsic contaminations. Therefore, a number of measurements were performed with the PTFE used for the construction of the XENON100 TPC (entries 15–16 in Table 1). No evidence for radioactive contaminants in the PTFE has been found within the sensitivity of the used spectrometer and only upper limits could be derived. In particular the contamination with α-emitters is found to be <0.1 mBq/kg for ^{232}Th and <0.06 mBq/kg for ^{226}Ra. Other samples of PTFE from different suppliers were measured (with a lower sensitivity) and found to have radioactive contaminations below 2 mBq/kg (entries 17–19 in Table 1).

Because of their small mass, two plastic samples were screened using the ICP-MS technique described in Sect. 4: a polymethyl methacrylate (PMMA) optical fiber to guide blue light from a LED into XENON100 for photosensor calibration (entry 41) and a thin PTFE sheet used as a light reflector (entry 17). The PTFE sheet has a radioactive contamination well within the XENON100 radioactivity requirements. Although the optical fiber exhibits a higher radioactivity than other plastic samples its contribution to the XENON100 background is negligible with respect to other samples, given its very small mass (10 g total).

5.3. R8520-06 Hamamatsu PMTs

Among the most important samples presented in this paper are the R8520-06-Al square $1'' \times 1''$ photomultiplier tubes (PMTs) from *Hamamatsu*. They are the light sensors chosen for XENON100 and therefore a central part of the detector. Given their proximity to the target volume and their nature of being a composite, fully assembled object, they are one of the dominating background sources. In order to determine the contribution of the PMTs to the overall background, and to reject possible "hot" tubes, a large fraction of the PMTs installed in the detector has been screened (entries 20–36 in Table 1) in the various facilities.

In order to fulfill the design requirements of XENON100, the manufacturer of the PMTs has assured that the components used for the production of the various PMT batches always have the same controlled origin. Nevertheless, some of the processes or working conditions in the production of the components might differ. Therefore, the PMTs have been subdivided in groups of typically 10-20 PMTs with tubes from the same production batch. The different groups have been screened independently to cross check their intrinsic radioactive contamination. Some batches have been discarded because of their increased level of radioactivity (entries 22, 24 and 25), which does not fulfill the design requirement. The PMTs in batch 25 were a subsample of devices used in XENON10. They have not been re-used in XENON100 because of their high ^{60}Co and

---

[2]X10CrNiMoTi18-1.

Table 2: Summary of the measured activities of the individual parts of the *Hamamatsu* R8520-06 PMT. The last row gives the expected values for a single PMT based on the measurements (1-6) taking into account the mass model, given in the second column of the Table.

PMT Component	Mass g	^{238}U mBq/kg	mBq/PMT	^{232}Th mBq/kg	mBq/PMT	^{40}K mBq/kg	mBq/PMT	^{60}Co mBq/kg	mBq/PMT
1. Kovar Metal: main metal package	13	19(7)	0.25(9)	< 13	< 0.17	90(10)	1.2(1)	40(20)	0.5(3)
2. Borosilicate glass: used in stem	1	970(20)	0.97(2)	340(20)	0.34(2)	2300(200)	2.3(2)	< 10	< 0.01
3. Ceramic: spacer between electrodes	0.04	780(20)	0.031(1)	260(20)	0.010(1)	800(100)	0.032(4)	< 12	$< 4.8 \times 10^{-4}$
4. Aluminum: sealing between quartz window and metal package	0.1	17(8)	0.0017(8)	370(20)	0.37(2)	5(2)	0.0005(2)	< 0.27	$< 2.7 \times 10^{-5}$
5. Stainless Steel: electrodes	7	19(7)	0.13(5)	18(8)	0.13(6)	0.15(2)	1.1(1)	12(5)	0.08(3)
6. Glass (synthetic silica): window	2	<0.5	< 0.001	< 1.8	< 0.0036	18(3)	0.036(6)	< 0.1	$< 2 \times 10^{-4}$
R8520-06-AL (total)	23.14		1.4(2)		0.85(7)		4.6(2)		0.6(3)

^{137}Cs content. All other screened PMT batches met the radioactivity requirements and were installed in the detector.

In order to have a detailed characterization of this PMT model and the possibility to improve the radioactivity in collaboration with *Hamamatsu*, all components of the R8520 PMT type used in XENON10 [27] have been screened individually. The results are given in Table 2.

According to the PMT mass model provided by *Hamamatsu*, (see second column of Table 2), the main components responsible for the overall PMT radioactivity have been identified: these are the metal package and the stem pins (made of Kovar metal which has a small thermal expansion coefficient), the borosilicate glass in the stem and the stainless steel electrodes. The table shows the contributions of the single components to the overall PMT radioactivity. Knowing the constituents dominating the overall radioactivity allows to select other materials, or materials processed in a different way, to use them in the development of new photosensors. This is important for the next generation of rare event search experiments where the background requirements are even more demanding.

The predicted activities for a single PMT, based on these measurements of the individual components, are given in the last row of Table 2. The numbers have to be compared with entries 20–36 of Table 1. For ^{238}U and ^{232}Th the predictions are higher than the average of the PMTs used in XENON100, but somewhat lower in ^{60}Co and ^{40}K. However, since the individual parts were not from the batches used in XENON100, and the disagreement is only a little larger than the uncertainties, this is an acceptable result.

5.4. Other samples

New photosensors with a larger active area (entries 37–39 in Table 1) have also been examined as they are interesting for the next generation LXe detectors such as XENON1T [28].

Special effort went into the design of the voltage divider circuit (bases) for the R8520-06 PMTs used in XENON100. The components (surface mount resistors and capacitors on a Cirlex substrate) have been reduced in mass and number and have been selected for lowest possible radioactive contaminations (entry 40 in Table 1). However, the contribution of the bases to the total background at low energies is still 10% of that from the PMTs [15]. The cables for the PMT signal (RG174, RG174, with the outer plastic insulation removed) and high voltage (silver coated, kapton insulated) have also been measured (entries 42 and 43). Given the rather small amount used in XENON100, their impact on the overall background is negligible.

Finally, another sample screened within the scope of this paper is the concrete used to build the underground laboratory. Two samples were taken from the wall and from the floor surrounding the XENON100 installation. The precise knowledge of the concrete's radioactive contaminations allows to calculate the expected neutron flux from (α, n) and spontaneous fission reactions in the material. The results measured with the Gator facility (entries 48, 49) agree with measurements of the background γ-flux at the same location [30].

5.5. Location of the screened components in XENON100

This section summarizes the location of the screened materials, as listed in Table 1, in XENON100. The detector is a position-sensitive TPC using liquid xenon (LXe) as target material. The light signals are detected by two arrays (on top and bottom of the detector) of *Hamamatsu* R8520-06 PMTs (entries 20–36). The LXe volume outside the TPC is also instrumented with PMTs in order to act as an active veto. All PMTs are mounted on voltage dividers (entry 40) and connected with coaxial (signal, entry 42) and single wire cables (high voltage, entry 43) to the feedthroughs (entry 46). These are placed outside the shield because of their higher radioactivity level. The sensitive target can be "fiducialized" to suppress the background by only keeping the inner core of the detector for the science analysis, exploiting the good self shielding properties of the LXe.

In order to suppress the γ-background from the laboratory environment (mainly from concrete [30], entries 48 and 49), the detector is placed inside a passive shield. It is made from lead (15 cm "normal" lead, entries 1 and 2, followed by 5 cm lead low in ^{210}Pb, entries 3 and 4), 20 cm polyethylene (entries 12–14) and 5 cm OFHC copper (entry 5). The whole shield sits

on a 25 cm slab of polyethylene and is additionally shielded against neutrons with 20 cm water on 3 sides and on the top.

The detector is installed in a double-walled cryostat made from low radioactivity stainless steel (entries 7-10). The LXe target volume is enclosed by a PTFE cylinder (entry 16) of ~15 cm radius and ~30 cm height. Copper wires, wound around the TPC and connected with resistors (entry 44), ensure electric field homogeneity. The PTFE panels are stabilized using rings of OFHC copper (entry 6). The same copper supports the PMTs on the bottom of the detector and all PMTs in the active LXe veto. The PMTs above the target are resting in a PTFE structure (entry 16) and fixed by smaller copper rings (entry 6). Everything is held together with stainless steel screws (entry 11). In order to improve the light collection in the active LXe veto volume the cryostat wall is covered by a thin PTFE sheet (entry 17).

A complete study of the XENON100 background has been published in [15]. It uses the screening results reported here as input values.

6. Summary

The materials used to construct experiments for rare event searches have to be selected in order to achieve the lowest possible radioactive background. This paper presents the results from the radioactivity screening campaign for XENON100, which aims to directly detect WIMP Dark Matter.

More than 20 different materials have been examined, mostly using low background HPGe detectors, but also applying mass spectrometry. In many cases, several batches of samples have been screened to check systematics or because the material properties were slighly different (different production batches, thickness, etc.). All results are given in Table 1, which might be very useful for other experiments searching for rare events. For this reason, we also provide the supplier for all samples.

These results have been used in a study to predict the electromagnetic background of XENON100 [15]. By comparing the measured energy spectrum between threshold and 2700 keV to a detailed Monte Carlo analysis, it is verified that the background design goal of $< 10^{-2}$ events keV^{-1} kg^{-1} day^{-1} has indeed been reached. Of all running direct Dark Matter detection experiments, XENON100 has the lowest electromagnetic background. This has already allowed to set a competitive limit on spin-independent WIMP-nucleon interactions with only a few days of measuring time [11, 12].

A detailed study of the intrinsic radioactive contamination of the *Hamamatsu* R8520-06 PMT, the light sensor used in XENON, has also been presented. The screening of individual PMT components provides information about which parts have to be modified in order to further decrease the radioactivity level. Almost equally important are the results obtained for the PTFE used for the XENON100 TPC, which is one of the purest PTFE samples ever reported in the literature.

References

[1] W. Freedman and M. Turner, Rev. Mod. Phys., **75** (2003) 1433.
[2] D. Clowe et al., ApJ, **648** (2006) 109.
[3] M.J. Jee et al., arXiv:0705.2171 (2007).
[4] R. J. Gaitskell, Ann. Rev. Nucl. Part. Sci., **54** (2004) 315.
[5] G. Chardin in "Cryogenic Particle Detection", editor C. Enss, Springer, Heidelberg, 2005.
[6] L. Baudis, Int. J. Mod. Phys. A **21** (2006) 1925.
[7] A. Bottino et al., Phys. Rev.**D 69** (2004) 315.
[8] J. Ellis et al., Phys. Rev.**D 71** (2005) 095007.
[9] H. C. Cheng et al., Phys. Rev. Lett. **89** (2002) 211301.
[10] A. Birkedal-Hansen and J. G. Wacker, Phys. Rev.**G69** (2004) 065022.
[11] E. Aprile et al. [XENON100], Phys. Rev. Lett. **105**, (2010) 131302.
[12] E. Aprile et al. [XENON100], arXiv:1103.0303 (2011).
[13] A.I. Bolozdynya, *Nucl. Instr. and Meth. in Phys. Res. A* **422** (1999) 314.
[14] E. Aprile et al., Phys. Rev. Lett. 97 (2006) 081302.
[15] E. Aprile *et al.* [XENON100 Collaboration], arXiv:1101.3866 (2011).
[16] L. Baudis et al., arXiv:1103.2125 (2011).
[17] C. Arpesella, Appl. Radiat. Isot. **9/10** (1996) 991.
[18] H. Neder, G. Heusser and M. Laubenstein Appl. Rad. Isot., **53** (2000) 191.
[19] G. Heusser, Annu. Rev. Nucl. Part. Sci. **45** (1995) 543.
[20] S. Agostinelli *et al.*, Nucl. Instrum. Meth. A **506** 250-303 (2003).
[21] G.F. Knoll, Radiation Detection and Measurement, John Wiley and Sons (2000).
[22] C. Hurtgen et al., Appl. Radiat. Isot. **53** (2000) 45.
[23] M. Heisel, F. Kaether and H. Simgen, Appl. Rad. Isot. **67** (2009) 741.
[24] P. Gaines, 2003. "Reliable measurement. A Guidebook for Trace Analyst." Inorganic Ventures Publication, January 2002, June 2003.
[25] W. Maneschg *et al.*, Nucl. Instr. and Meth. in Phys. Res. A **593** (2008) 448.
[26] M. Yamashita *et al.*, NIM A **535** (2004) 692.
[27] J. Angle et al. [XENON10], Phys. Rev. Lett. **100** (2008) 021303.
[28] A. Teymourian et al., arXiv:1103.3689v1 (2011).
[29] E.B. Norman *et al.* Phys. Rev. C **30** (1984) 1339.
[30] M. Haffke et al., arXiv:1101.5298 (2011).